Journal of Non-Crystalline Solids 603 (2023) 122097

Contents lists available at ScienceDirect

Journal of Non-Crystalline Solids

journal homepage: www.elsevier.com/locate/jnoncrysol

Tungsten gallium-phosphate glasses as promising intrinsic scintillators

Thiago A. Lodi [a,*], Gustavo Galleani [a], Leonnam G. Merízio [a], Luiz G. Jacobsohn [b], Valmor R. Mastelaro [a], Andrea S.S. de Camargo [a,*]

[a] São Carlos Institute of Physics, University of São Paulo, São Carlos, SP, 13566-590, Brazil
[b] Department of Materials Science and Engineering, Clemson University, Clemson, SC, 29634, United States of America

ARTICLE INFO

Keywords:
Tungsten gallium-phosphate glass
Intrinsic scintillator
Radioluminescence

ABSTRACT

Tungsten gallium-phosphate glasses with composition $NaPO_3$-$20Ga_2O_3$-xNa_2WO_4 (x = 0, 1, 3, 5 and 10% mol) were synthesized by the melt-quenching technique with high chemical stability and excellent optical properties, and evaluated as potential intrinsic glass scintillators. Fourier-transform infrared measurements showed a decrease in the amount of OH^- groups for increasing Na_2WO_4 contents, while X-ray photoelectron spectroscopy revealed the presence of sole W^{6+} species. Optical transmission measurements showed a high level of transmittance (~90%) over a broad spectral range (400 to 2500 nm). Luminescence was found to correspond to a broad emission characteristic of the WO_4^{2-} complex that can be excited by ultraviolet and X-rays with average lifetimes ranging from 32 to 20 μs. At cryogenic temperatures, the NaPGaW glasses showed a significant increase in the luminescence emission.

1. Introduction

Ionizing radiation, such as X-rays, is present in medical, scientific and security applications such as radiography, crystallography, elemental identification and surveillance [1]. Particularly, the materials science research has been greatly benefited through the opening of a new era of X-rays imaging analysis [2]. In order to ensure effective and safe use of X-rays, proper handling, detection, and dose determination are paramount. Concerning X-ray detection, most of the detectors are based on the scintillation phenomenon which consists in the conversion of the ionizing radiation into ultraviolet (UV)-visible light [3]. Scintillation can be categorized as either extrinsic when optically active ions are doped into the scintillator host material, or intrinsic when functional groups within the structure of the material are responsible for the light emission. Whichever the mechanism, the visible emission from the scintillator is collected and converted into an electrical signal by highly sensitive photomultiplier tubes (PMT) [2,4].

Traditional crystalline scintillators present optimum performance but, nonetheless, the manufacturing methods of single crystals are usually complex, costly, time-consuming and limited with respect to obtaining large sized materials, hindering widespread commercial use of scintillators. The advantages of the chemical stability, lower fabrication cost, already-in-place high-volume industrial fabrication of glasses, in various sizes and shapes, are strong incentives for the development of new glass scintillators [5]. Glass compositions containing tungsten oxy-anionic complexes such as $[WO_6]^{6-}$ and $[WO_4]^{2-}$ can be a particularly promising alternative for monocrystalline intrinsic scintillators. Their emission generates a high number of photons over a broad spectral region possibly resulting in superior signal-to-noise ratios and short integration times. To the best of our knowledge, tungsten gallium-phosphate glasses have not been investigated as scintillators. In this work, we report on the fabrication and characterization of glasses in the compositional system $NaPO_3$ - Ga_2O_3 - Na_2WO_4 with variable concentration of tungsten as potential scintillators for X-ray detection.

2. Experimental procedure

Tungsten gallium-phosphate glasses, hereafter referred to as NaPGaW, were prepared via the melt-quenching technique according to the stoichiometric compositions (80 - x) $NaPO_3$ - 20 Ga_2O_3 - x Na_2WO_4 (x = 0, 1, 3, 5 and 10% mol) as summarized in Table 1. The powders of the raw materials were thoroughly mixed in an agate mortar and melted in a platinum crucible in a furnace at 1000 - 1050 °C, depending on the Na_2WO_4 content. Approximately 8 × 8 mm^2 and 2.5 mm thick polished plates of the NaPGaW glasses were used for the optical transmittance, absorption, Fourier-transform infrared (-FT-IR) absorption, photoluminescence excitation (PLE) and emission (PL) measurements at room temperature. For the photophysical characterization, we secured that all

* Corresponding authors.
E-mail addresses: augustolodi@usp.br (T.A. Lodi), andreasc@ifsc.usp.br (A.S.S. de Camargo).

https://doi.org/10.1016/j.jnoncrysol.2022.122097
Received 18 September 2022; Received in revised form 14 December 2022; Accepted 17 December 2022
Available online 22 December 2022

Table 1
Glass label, nominal composition (mol%) and energy gap (eV) of NaPGa and NaPGaW glasses.

Glass label	Nominal composition (mol%)		
	$NaPO_3$	Ga_2O_3	Na_2WO_4
NaPGa	80	20	-
NaPGaW1	79	20	1
NaPGaW3	77	20	3
NaPGaW5	75	20	5
NaPGaW10	70	20	10

the studied samples had the same dimensions. For the X-ray photoelectron spectroscopy (XPS) and radioluminescence (RL) measurements, the glasses were ground and used in the powder form.

FT-IR analysis was carried out using an Agilent Cary 630 spectrometer operating in attenuated total reflection (ATR) mode. XPS analysis was performed with a ScientaOmicron ESCA+ XPS spectrometer equipped with a high-performance hemispherical analyzer (EAC2000) with monochromatic Al Kα radiation ($h\nu = 1486.6$ eV) as the excitation source. XPS spectra were recorded at constant pass energy of 20 eV with 0.05 eV per step for the high-resolution spectra and the data were analyzed using the CASA XPS software. The optical transmission and absorption measurements were carried out using a UV–Vis-NIR Perkin-Elmer double-beam spectrometer model Lambda 1050 in the range 250-2500 nm, with a spectral resolution of 1 nm. The PLE and PL spectra of NaPGaW glasses were recorded with a HORIBA Jobin Yvon spectrofluorimeter model Fluorolog-3 equipped with a 450 W CW Xenon arc lamp as the excitation source. The excited state lifetime values were measured in the same spectrofluorimeter using a pulsed Xe lamp, and the decay curves were analyzed using the DAS6 software. Temperature-dependent experiments (80-300 K) were carried using the same equipment coupled to a temperature controller model Linkam THMS600. RL measurements were recorded with a Freiberg Instruments Lexsyg Research spectrofluorimeter using a Varian Medical Systems VF-50J X-ray tube with a tungsten target as the X-ray source. More details can be found in Ref. [6].

3. Results and discussion

Fig. 1(a) shows a photograph of a representative NaPGaW glass sample in ambient light highlighting its high optical transmittance, and 1(b) shows the luminescence of the whole series of glasses under UV excitation where the glasses were placed in ascending order of Na_2WO_4 content (left to right). The first glass shown on the left in Fig. 1(b) does not have Na_2WO_4 in its composition. All NaPGaW glasses are colorless, transparent, and are non-hygroscopic.

3.1. Infrared absorption spectroscopy (FT-IR)

FT-IR spectra of NaPGa and NaPGaW glasses in the frequency region between 4000 and 700 cm^{-1} are presented in Fig. 2. A broad band centered at approximately 3300 cm^{-1} (a) can be observed, which is attributed to symmetric stretching of OH^- groups present in the glass structure [4]. In the inset, a magnified view of this region is presented, evidencing the decrease in this band as a function of Na_2WO_4 content. This is an indication of increased chemical stability of the NaPGaW glasses for increasing Na_2WO_4 contents. The band located between 2300 and 2200 cm^{-1}, observed in the spectra of all glasses, is assigned to molecular CO_2 present in the atmosphere [7]. The band centered at 1640 cm^{-1} (b) is assigned to the bending vibration mode of OH^- groups [4,8]. The low relative intensity of the OH^- related bands indicates the excellent quality of the NaPGaW glasses. In the frequency range 1300 to 650 cm^{-1}, four bands can be observed. The band at 1150 cm^{-1} (c), evident in the spectra of the NaPGa, NaPGaW5 and NaPGaW10 samples, is attributed to the asymmetric vibration of PO_4 units. The band at 1050 cm^{-1} (d) is attributed to symmetric stretching modes of tetrahedral Q^0 groups $(PO_4)^{3-}$ [9], while the band at 870 cm^{-1} is assigned to P-O-P asymmetric bending vibrations. These last three bands do not change significantly with increasing Na_2WO_4 content. A different behavior can be noticed at 750 cm^{-1}, a band attributed to the presence of symmetric stretching modes of the bridging oxygen (O_B) bonded to a phosphorus atom in a Q^2 phosphate tetrahedron [10]. This band disappears when Na_2WO_4 is added, indicating that the addition of Na_2WO_4 favors the depolymerization of the phosphate network.

3.2. X-ray photoelectron spectroscopy (XPS)

Seeking for a better comprehension of the origin of the broadband emission of NaPGaW glasses (discussed below), an investigation of the

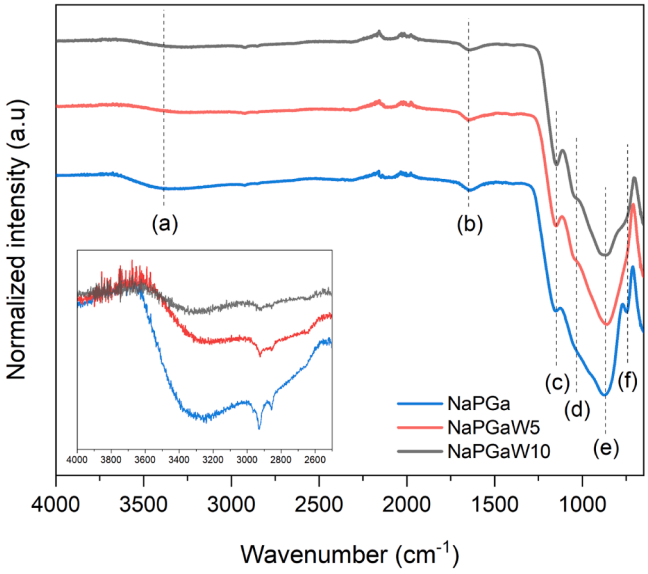

Fig. 2. FTIR spectra of representative glasses. The inset shows a magnified view of the region where the stretching mode of OH^- is located.

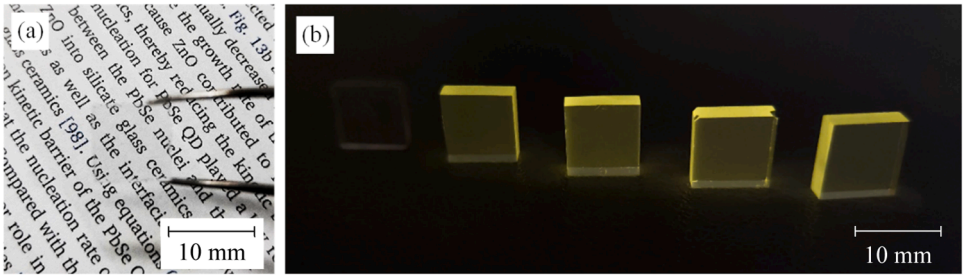

Fig. 1. Photographs of the NaPGa and NaPGaW glass samples: (a) a representative glass in ambient light and (b) the whole series of luminescent glasses under UV light (300 nm).

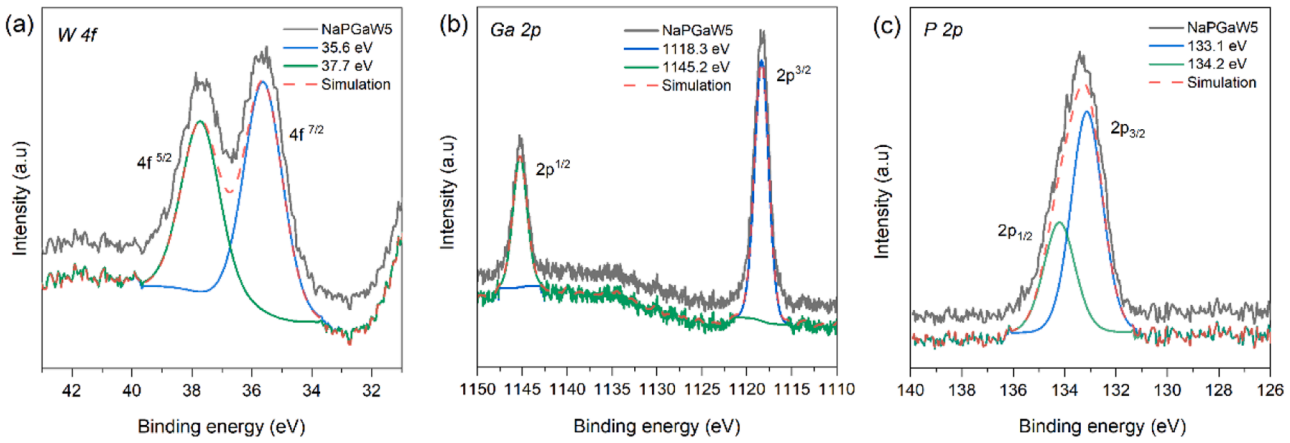

Fig. 3. XPS high-resolution spectra of a) tungsten 4f, b) gallium 2p, and c) phosphor 2p of the NaPGaW5 glass.

Table 2
Peak positions (in eV) obtained from curve fitting of the P 2p, Ga 2p, and W 4f XPS spectra of the NaPGa and NaPGaW glasses.

Glass label	Peak position (eV)		
	W 4f	Ga 2p	P 2p
NaPGa	-	1144.8	133.9
		1118.0	132.9
NaPGaW1	37.6	1145.1	134.0
	35.5	1118.2	133.0
NaPGaW3	37.7	1145.2	134.0
	35.5	1118.3	133.0
NaPGaW5	37.7	1145.2	134.1
	35.6	1118.3	133.2
NaPGaW10	37.6	1145.2	134.0
	35.5	1118.3	133.0

samples by high-resolution XPS was carried out. Fig. 3 shows the W 4f (a), Ga 2p (b), and P 2p (c) XPS spectra of the representative glass NaPGaW5. In the XPS spectrum of W 4f level, two peaks centered at 37.7 and 35.6 eV are fitted by Lorentzian-Gaussian functions and are attributed to the W $4f_{5/2}$ and W $4f_{7/2}$ levels of the W^{6+} ion, respectively. The presence of other oxidation states of W was not observed, confirming that the broadband observed in the visible region is attributed to hexavalent tungsten. Furthermore, Fig.s 3 (b) and (c) presents the XPS spectra of the Ga 2p and P 2p core levels, respectively. For the Ga 2p core level, two peaks centered at 1145.2 and 1118.3 eV can be observed, which correspond to, respectively, the binding energy (E_b) of electrons in the $2p_{1/2}$ and $2p_{3/2}$ levels of gallium in the Ga^{3+} valence state [11]. The XPS spectrum of the P 2p core level (see Fig. 3c), in turn, is decomposed into two peaks with $E_b = 134.2$ and 133.1 eV and with an energy difference between these peaks $\Delta E_b = 0.9$ eV, ΔE_b characteristic of $2p_{1/2}$ and P $2p_{3/2}$ [12]. The binding energies of these elements for all glass samples can be found in Table 2, which clearly shows that there are no significant changes as a function of the Na_2WO_4 content. Interestingly, we did not observe any significant change in the W 4f spectrum of the NaPGaW10 glass that could corroborate our hypothesis of the presence of different W species in this glass in comparison to the other glasses with lower concentrations of Na_2WO_4. We tentatively attribute this to the small concentration of the other W species coupled to the sensitivity of the XPS detection system.

3.3. UV-Vis-IR absorption spectroscopy

Fig. 4 shows the optical transmission spectra of NaPGaWx (x = 0, 1,

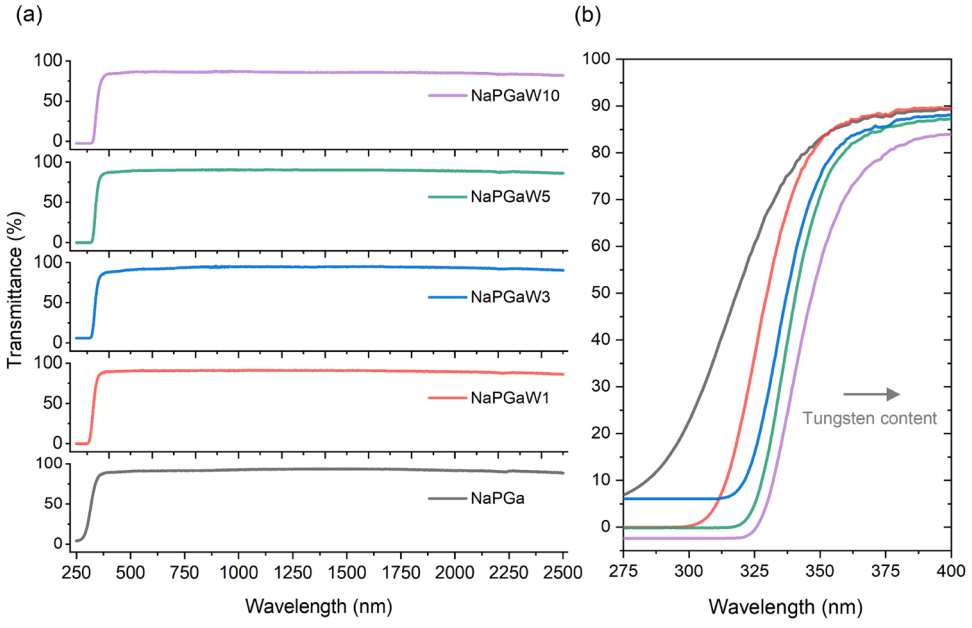

Fig. 4. (a) Transmittance spectra of the NaPGaW glasses in the UV, visible, and near-infrared ranges and (b) redshift as a function of tungsten content.

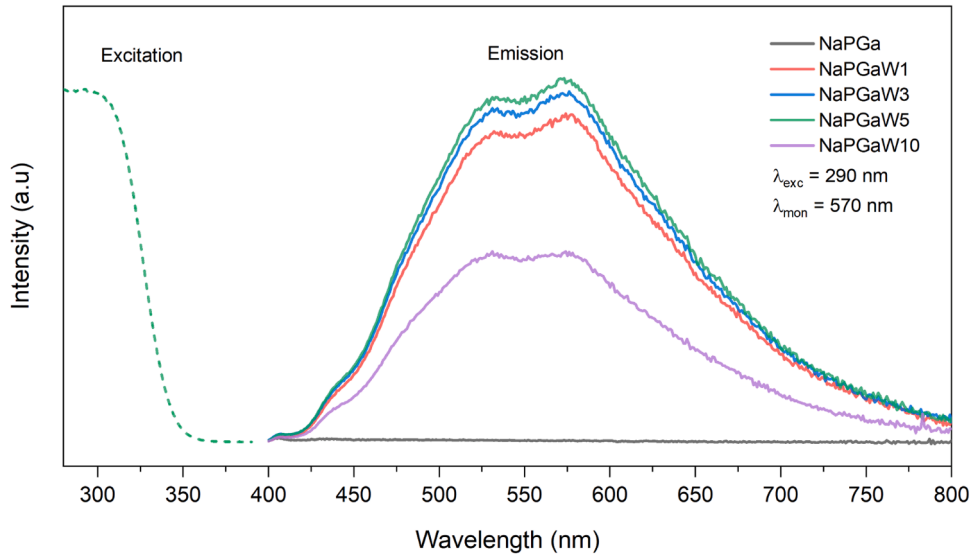

Fig. 5. PLE excitation spectrum of NaPGaW5 monitoring the emission at 570 nm (dashed green line), and PL emission of NaPGa and NaPGaW glasses measured under excitation at 290 nm (solid lines).

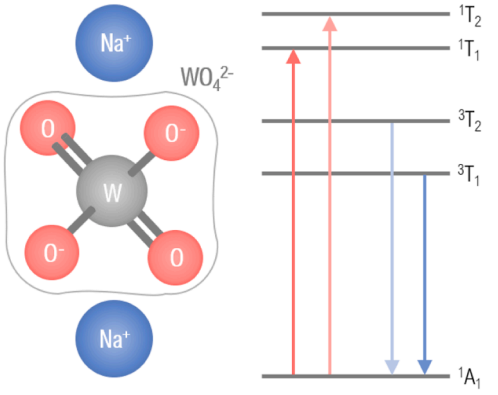

Fig. 6. Left: Structure of Na_2WO_4 and WO_4^{2-} tetrahedra. Right: Schematic energy level diagram (not to scale) of the emission processes in the WO_4^{2-} complex in the scheelite structure.

3, 5 and 10 mol%) glasses in the UV-Vis-IR spectral region. All the samples exhibit high transparency (≈ 90%) in the 400 to 2500 nm range, indicating that these glasses are suitable as hosts for various luminescent dopant ions. By increasing the content of Na_2WO_4, the absorption edge of the NaPGaW glasses shifts towards longer wavelengths (*cf.* Fig. 4). This shift can be explained by the increase of the covalent character of the vitreous network, which is attributed to the insertion of WO_n polyhedra between PO_4 units of the phosphate network [13]. Since the optical energy gap arises from the electronic transitions from the conduction band to the valence band, it can be inferred that the progressive incorporation of Na_2WO_4 in the vitreous network reduces the optical energy gap between these bands.

3.4. Photoluminesce excitation and emission

The photoluminescence excitation and emission spectra of NaPGa and NaPGaW glasses at room temperature are shown in Fig. 5. It is noted that the excitation spectra obtained by monitoring the emission at 570 nm could only be collected starting at 280 nm due to limitations of the spectrofluorimeter detector. Consequently, only the excitation spectrum of the NaPGaW5 glass is presented for illustrative purposes.

In phosphors, crystals, and films of tungstates like $CaWO_4$, $BaWO_4$, $SrWO_4$, and $PbWO_4$ [14–16], the excitation band covers a broad range within the 200 ~ 350 nm spectral region, peaking at about 280 nm. This excitation band is ascribed to the charge transfer band (CTB) from the oxygen 2p orbitals to one of the empty tungsten 5d orbitals within the WO_4^{2-} groups. This is consistent with our results shown in Fig. 5.

The emission spectra of the NaPGa and NaPGaW glasses were collected upon excitation at 290 nm (solids lines in Fig. 6). The Na_2WO_4 free glass (black line) does not present emission in this region, corroborating that the emission observed in the other glasses is related to the tungstate groups. The NaPGaW*x* glasses with $x = 1$, 3, 5, and 10 mol% Na_2WO_4 present a broad emission in the spectral range 420 to 800 nm. The origin of the broad visible emission band presented by tungstates, as well as molybdates, is quite polemical in the literature. It is generally accepted, however, that the emission of tungstates and molybdates like Na_2WO_4, $CaWO_4$, and $CaMoO_4$ with scheelite structure results from the radiative recombination of self-trapped excitons (STEs) localized at WO_4^{2-} molecular ions [16–18]. It is also known that Na_2WO_4 is built up by isolated tetrahedral WO_4^{2-} units and that all the bonds in the structure are terminal (i.e., two W=O and two W-O^- [19]), as schematized in Fig. 6. As indicated in the energy level diagram of Fig. 6, when excited by short wavelength radiation ($^1A_1 \rightarrow {}^1T_1, {}^1T_2$ transitions) the WO_4^{2-} complex yields two emissions at 460 nm and at 520 nm. The blue emission ($^3T_2 \rightarrow {}^1A_1$ transition) is attributed to the WO_4 tetrahedron while the green one ($^3T_1 \rightarrow {}^1A_1$) is attributed to WO_3 defect centers associated with oxygen vacancies, however, sometimes it is attributed to intrinsic transitions in the WO_4^{2-} complex [20]. These two emissions are clearly present in the spectra of NaPGaW glasses. Furthermore, a component between 600 - 650 nm also seems to be convoluted in the spectra of Fig. 5, which has been previously observed and is believed to originate from the transitions in a WO_3 group or higher tungstate complexes, which once again indicates the presence of a variety of tungsten species in the glasses [15,20].

Another interesting aspect shown in Fig. 5 is the fact that the intensity of the broad emission band increases with increasing concentration of Na_2WO_4 up to 5 mol%, and then decreases for higher concentrations. We hypothesize that for higher tungsten concentrations, the formation of additional anionic species such as the complex W_2O_7 is highly probable and the variations in intensity are related to the relative contributions of these different species.

To evaluate the colorimetric performance of the NaPGaW glasses, the emission colors were analyzed using the Commission Internationale de l'Eclairage (CIE, 1931) chromaticity coordinates (*x*, *y*). For the most

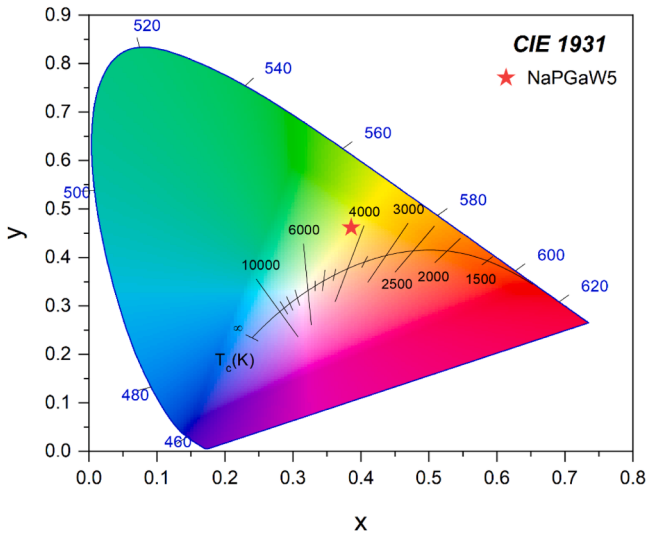

Fig. 7. CIE 1931 diagram of the representative NaPGaW5 glass.

emissive NaPGaW5 glass, the CIE coordinates are shown in Fig. 7. They are $x = 0.38$ and $y = 0.46$ while the correlated color temperature (CCT) equals 4300 K. The other glasses showed no significant differences in the values of chromaticity coordinates and color temperature and thus are not shown in Fig. 7.

Motivated by an increasing number of applications of scintillators at low temperatures, like cryogenic experiments searching for rare events [21–23], we investigated the luminescence of NaPGaW glasses over a wide temperature range, as the luminescence resulting from STEs is a process that exhibits strong temperature dependence. Fig. 8(a) shows the variation of the PL emission response of NaPGaW5 glass over the 80-300 K temperature range. At lower temperatures, the lack of thermal energy favors radiative recombination and higher emission intensities are expected. Fig. 8(b) shows the integrated emission intensity as a function of the temperature for the NaPGaW5 glass. At 80 K, the integrated intensity is about 16x higher than at room temperature. In Fig. 8 (c), it is possible to observe that a progressive inhomogeneous broadening of the band on the high energy side takes place for temperatures above 80 K indicating vibronic coupling [24].

3.5. Luminescence decay lifetimes

The luminescence decay curve of the NaPGaW5 glass measured at room temperature is shown in Fig. S2 along with the curve of the pulsed laser decay (at 290 nm). Considering that the broad emission has contributions from more than one luminescence center, the lifetime decay curves were interpreted as a distribution of decay times. The decay curves were fitted with three exponentials and taking into account the different weights, with the resulting lifetime values ranging from 32 to 20 μs being considered as average values (Fig. 9). Overall, the average lifetime decreases for higher Na_2WO_4 contents, in agreement with previous reports in the literature for tungstate glasses and crystals [25,26]. Notably, a good compromise between emission intensity and a short lifetime is achieved by the NaPGaW5 glass.

3.6. Radioluminescence

To evaluate the capability of NaPGaW glasses to detect X-rays, RL

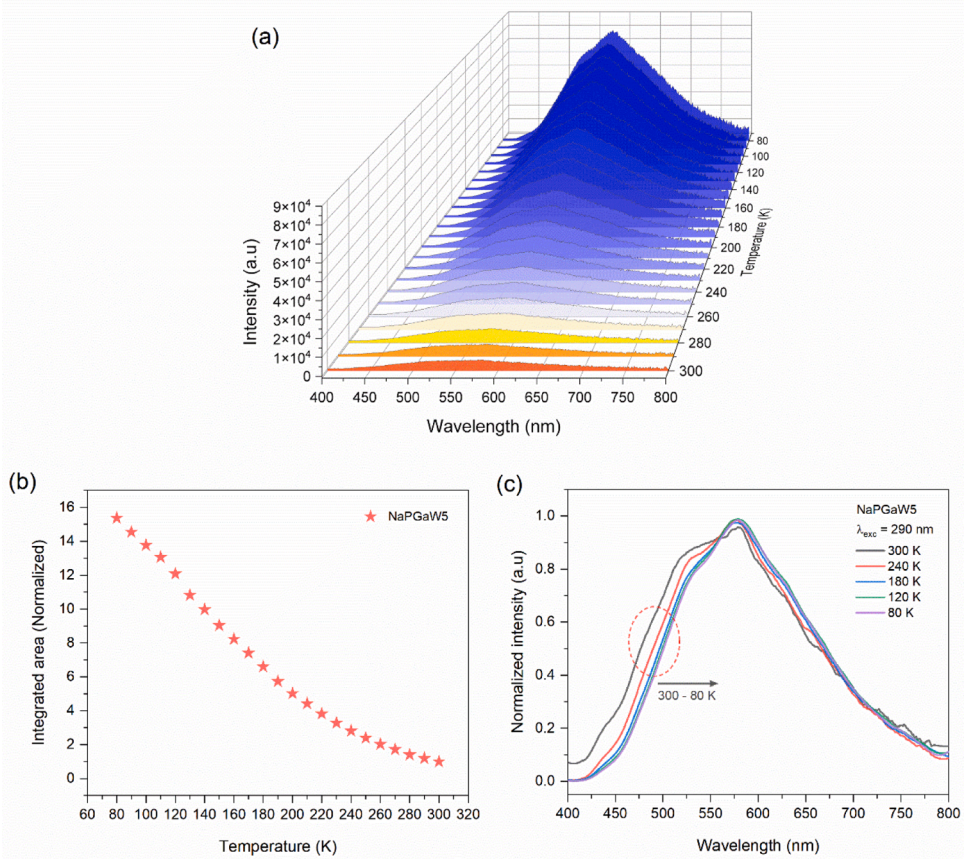

Fig. 8. (a) Temperature dependence of the emission of representative glass NaPGaW5 in the 300 – 80 K temperature range under 290 nm excitation. (b) Integrated area of the broad emission band of the NaPGaW5 glass as a function of temperature (80-300 K). (c) Normalized PL emission of the NaPGaW5 glass as a function of the temperature.

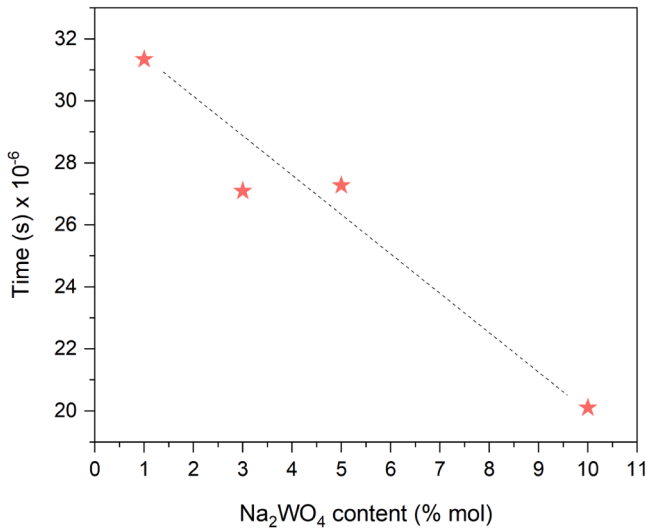

Fig. 9. Average lifetime values as a function of the Na_2WO_4 content. The dash-dotted line in the figure is a guide for the eyes.

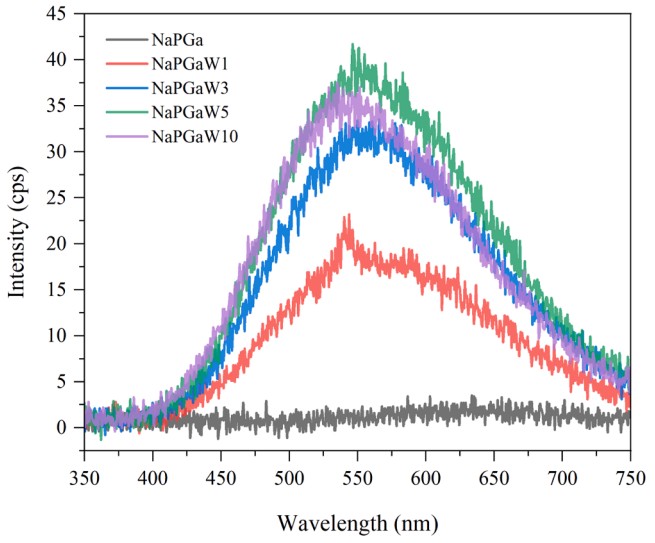

Fig. 10. Radioluminescence spectra of the NaPGaW glasses under X-ray excitation.

spectra of all samples were obtained at room temperature, as shown in Fig. 10. A broad band centered at approximately 550 nm was observed, similar to the one observed upon UV excitation. As discussed in the UV case, the NaPGa glass did not present emission in this spectral region. Contrary to the case of the $PbWO_4$ scintillator, in which the emission mechanism arises from Pb^{2+} and WO_4^{2-} ions and energy transfer mechanisms between radiating centers lead to a fast decaying but low intensity scintillation at room temperature, in the case of the present glasses the emission originates from the radiative recombination of self-trapped excitons (STEs) localized at WO_4^{2-} ions [27,28]. The emission intensity increases with increasing concentration of tungsten oxide up to 5 mol% and then decreases for higher concentrations, as also observed for UV excitation. Whatever the excitation mechanism, UV or X-rays, the emission bands of the NaPGaW glasses match very well with the spectral sensitivity region of Si photodetectors and photomultipler tubes, being in the same spectral region of the emission of the well and long known scintillators $Bi_4Ge_3O_{12}$ (BGO) and $CdWO_4$ [28,29].

Although it is not the aim of this work to propose our glasses as promising substitutes for well-established commercial scintillator crystals as BGO, a comparison of emission intensities of samples with very similar dimension and under the same experimental conditions (Fig. S2) indicates that the emission of the glasses is incomparably lower than the crystal, which is not surprising, given the different compositions and nature of the materials. Still, this result indicates that, given the previously mentioned cost and production constraints of crystal obtainment, there are many opportunities for the development of glass scintillators with, so far, very few reports in the literature. As to the new tungsten gallium-phosphate glasses, they might find use in specific applications not requiring high levels of intensity.

4. Conclusions

Tungsten gallium-phosphate glasses were successfully synthesized by the melt-quenching technique with high stability and excellent optical quality aiming at the application in scintillating detectors. The synthesized glasses present high optical transparency (~ 90%) in the 300-2000 nm region also enabling their use as transparent hosts for active dopant ions. XPS analysis indicate the sole or predominant presence of W^{6+}, in agreement with luminescence results, suggesting that WO_4^{2-} complexes are the luminophore. The NaPGaW glasses present a broad visible emission under UV and X-ray excitation ascribed to the radiative decay of self-trapped excitons characteristic of the WO_4^{2-} complexes. At cryogenic temperatures, the NaPGaW glasses showed enhanced luminescence intensity. The average luminescence decay time for the NaPGaW glasses is in the order of 20-32 μs, compatible with applications demanding a fast response. In summary, the results suggest the NaPGaW glasses to be a potential glass scintillator, specially at cryogenic temperatures.

CRediT authorship contribution statement

Thiago A. Lodi: Conceptualization, Methodology, Investigation, Data curation, Writing – original draft. **Gustavo Galleani:** Conceptualization, Data curation, Investigation, Writing – review & editing. **Leonnam G. Merízio:** Investigation, Data curation, Formal analysis, Writing – original draft. **Luiz G. Jacobsohn:** Investigation, Data curation, Writing – review & editing. **Valmor R. Mastelaro:** Investigation, Writing – review & editing, Supervision. **Andrea S.S. de Camargo:** Conceptualization, Writing – review & editing, Supervision, Funding acquisition.

Declaration of Competing Interest

The authors declare the following financial interests/personal relationships which may be considered as potential competing interests:

De Camargo, Andrea Simone Stucchi reports financial support was provided by State of Sao Paulo Research Foundation. Mastelaro, Valmor Roberto reports financial support was provided by National Council for Scientific and Technological Development. Jacobsohn, Luiz Gustavo reports financial support was provided by National Science Foundation. De Camargo, Andrea Simone Stucchi reports a relationship with University of São Paulo that includes: employment. Mastelaro, Valmor Roberto reports a relationship with University of São Paulo that includes: employment. Jacobsohn, Luiz Gustavo reports a relationship with Clemson University that includes: employment. None

Data availability

Data will be made available on request.

Acknowledgments

Authors would like to acknowledge the Brazilian funding agencies CAPES - Coordenação de Aperfeiçoamento de Pessoal de Nível Superior,

CNPq - Conselho Nacional de Desenvolvimento Científico e Tecnológico (Universal project 130562/2018-1) and FAPESP - Fundação de Amparo à Pesquisa do Estado de São Paulo (Process number 2013/07793-6, CEPID program). GG personally acknowledges a fellowship funding by FAPESP, (grant number 2018/03931-9). LGM personally acknowledges a fellowship funding by FAPESP, (grant number 2019/21770-5). L.G. Jacobsohn's work was supported by the National Science Foundation under Grant no. 1653016.

Supplementary materials

Supplementary material associated with this article can be found, in the online version, at doi:10.1016/j.jnoncrysol.2022.122097.

References

[1] P. Lecoq, A. Gektin, M. Korzhik, Inorganic Scintillators for Detector Systems, Second edi, Springer, Berlim, Germany, 2017.
[2] C.W.E. van E Delft, Inorganic scintillators in medical imaging, Phys. Med. Biol. 85 (2002) R85–R106, https://doi.org/10.1016/S0168-9002(03)01542-0.
[3] S.N. Ahmed, Physics and Engineering of Radiation Detection, 2015, 2º Edition.
[4] A.M. Abdelghany, A.H. Hammad, The effect of WO_3 dopant on the structural and optical properties of ZnO-P_2O_5 glass and the effect of gamma irradiation, J. Mol. Struct. 1081 (2015) 342–347, https://doi.org/10.1016/j.molstruc.2014.10.055.
[5] J.D. Musgraves, J. Hu, L. Calvez, Handbook of Glass, 2019, 1ª Edition.
[6] I.C. Pinto, G. Galleani, L.G. Jacobsohn, Y. Ledemi, Y. Messaddeq, A.S.S. de Camargo, Fluorophosphate glasses doped with Eu^{3+} and Dy^{3+} for X-ray radiography, J. Alloys Compd. 863 (2021), 158382, https://doi.org/10.1016/j.jallcom.2020.158382.
[7] L.G. Merízio, T.A. Lodi, E. Bonturim, A.S.S. de Camargo, Persistent luminescent phosphor-in-glass composites based on $NaPO_3$ – Ga_2O_3 glasses loaded with $Sr_2MgSi_2O_7$:Eu^{2+},Dy^{3+}, Opt. Mater. (Amst.) 134 (2022), 113046 https://doi.org/10.1016/j.optmat.2022.113046.
[8] M.A. Ouis, M.A. Azooz, H.A. Elbatal, Optical and infrared spectral investigations of cadmium zinc phosphate glasses doped with WO_3 or MoO_3 before and after subjecting to gamma irradiation, J. Non Cryst. Solid. 494 (2018) 31–39, https://doi.org/10.1016/j.jnoncrysol.2018.04.053.
[9] M. Lu, F. Wang, Q. Liao, K. Chen, J. Qin, S. Pan, FTIR spectra and thermal properties of TiO_2-doped iron phosphate glasses, J. Mol. Struct. 1081 (2015) 187–192, https://doi.org/10.1016/j.molstruc.2014.10.029.
[10] E. El-Meliegy, M.M. Farag, J.C. Knowles, Dissolution and drug release profiles of phosphate glasses doped with high valency oxides, J. Mater. Sci. Mater. Med. 27 (2016) 1–10, https://doi.org/10.1007/s10856-016-5711-8.
[11] K. Girija, S. Thirumalairajan, V.R. Mastelaro, D. Mangalaraj, Photocatalytic degradation of organic pollutants by shape selective synthesis of β-Ga_2O_3 microspheres constituted by nanospheres for environmental remediation, J. Mater. Chem. A Mater. 3 (2015) 2617–2627, https://doi.org/10.1039/c4ta05295a.
[12] Z. Wang, D. Kong, M. Wang, G. Wang, N. Li, D. Li, Sealing effect of surface porosity of Ti-P composite films on tinplates, RSC Adv. 9 (2019) 12990–12997, https://doi.org/10.1039/c8ra10523e.
[13] D. Manzani, R.G. Fernandes, Y. Messaddeq, S.J.L. Ribeiro, F.C. Cassanjes, G. Poirier, Thermal, structural and optical properties of new tungsten lead-pyrophosphate glasses, Opt. Mater. (Amst.) 33 (2011) 1862–1866, https://doi.org/10.1016/j.optmat.2011.02.041.
[14] V. Kumar, Z. Luo, A review on x-ray excited emission decay dynamics in inorganic scintillator materials, Photonics 8 (2021) 1–27, https://doi.org/10.3390/photonics8030071.
[15] Z. Lou, M. Cocivera, Cathodoluminescence of $CaWO_4$ and $SrWO_4$ thin films prepared by spray pyrolysis, Mater. Res. Bull. 37 (2002) 1573–1582, https://doi.org/10.1016/S0025-5408(02)00851-6.
[16] V. Yakovyna, Y. Zhydachevskii', V.B. Mikhailik, I. Solskii, D. Sugak, M. Vakiv, Effect of thermo-chemical treatments on the luminescence and scintillation properties of $CaWO_4$, Opt. Mater. (Amst.) 30 (2008) 1630–1634, https://doi.org/10.1016/j.optmat.2007.11.003.
[17] V.B. Mikhailik, H. Kraus, G. Miller, M.S. Mykhaylyk, D. Wahl, Luminescence of $CaWO_4$, $CaMoO_4$, and $ZnWO_4$ scintillating crystals under different excitations, J. Appl. Phys. 97 (2005), https://doi.org/10.1063/1.1872198.
[18] N. Ahmed, H. Kraus, H.J. Kim, V. Mokina, V. Tsiumra, A. Wagner, Y. Zhydachevskyy, V.B. Mykhaylyk, Characterisation of tungstate and molybdate crystals ABO_4 (A = Ca, Sr, Zn, Cd; B = W, Mo) for luminescence lifetime cryothermometry, Materialia (Oxf.) 4 (2018) 287–296, https://doi.org/10.1016/j.mtla.2018.09.039.
[19] G. Poirier, Y. Messaddeq, S.J.L. Ribeiro, M. Poulain, Structural study of tungstate fluorophosphate glasses by Raman and X-ray absorption spectroscopy, J. Solid State Chem. 178 (2005) 1533–1538, https://doi.org/10.1016/j.jssc.2004.10.032.
[20] A.B. Campos, A.Z. Simões, E. Longo, J.A. Varela, V.M. Longo, A.T. de Figueiredo, F. S. de Vicente, A.C. Hernandes, Mechanisms behind blue, green, and red photoluminescence emissions in $CaWO_4$ and $CaMoO_4$ powders, Appl. Phys. Lett. 91 (2007) 1–4, https://doi.org/10.1063/1.2766856.
[21] V.B. Mikhailik, S. Galkin, H. Kraus, V. Mokina, A. Hrytsak, V. Kapustianyk, M. Panasiuk, M. Rudko, V. Rudyk, ZnTe cryogenic scintillator, J. Lumin. 188 (2017) 600–603, https://doi.org/10.1016/j.jlumin.2017.05.021.
[22] D. Poda, Scintillation in low-temperature particle detectors, Physics (Switzerland) 3 (2021) 473–535, https://doi.org/10.3390/physics3030032.
[23] H. Kraus, V.B. Mikhailik, Y. Ramachers, D. Day, K.B. Hutton, J. Telfer, Feasibility study of a $ZnWO_4$ scintillator for exploiting materials signature in cryogenic WIMP dark matter searches, Phys. Lett., Sect. B: Nucl., Element. Particl. High-Energy Phys. 610 (2005) 37–44, https://doi.org/10.1016/j.physletb.2005.01.095.
[24] M. Fox, Optical Properties of Solids, Second Edi, Oxford University Press, 2010.
[25] H. Kraus, V.B. Mikhailik, D. Wahl, Multiple photon counting coincidence (MPCC) technique for scintillator characterisation and its application to studies of $CaWO_4$ and $ZnWO_4$ scintillators, Nucl. Instrum. Methods. Phys. Res. A 553 (2005) 522–534, https://doi.org/10.1016/j.nima.2005.07.011.
[26] T. Scheike, H. Segawa, S. Inoue, Y. Wada, Blue luminescence in the WO_3-P_2O_5-ZnO glass system, Opt. Mater. (Amst.) 34 (2012) 1488–1492, https://doi.org/10.1016/j.optmat.2012.03.014.
[27] P. Lecoq, I. Dafinei, E. Auffray, M. Schneegans, M.v. Korzhik, O.v. Missevitch, V. B. Pavlenko, A.A. Fedorov, A.N. Annenkov, V.L. Kostylev, V.D. Ligun, Lead tungstate ($PbWO_4$) scintillators for LHC EM calorimetry, Nucl. Inst. and Method. Phys. Res., A. 365 (1995) 291–298, https://doi.org/10.1016/0168-9002(95)00589-7.
[28] J.H. Ryu, J.W. Yoon, K.B. Shim, Blue luminescence of nanocrystalline $PbWO_4$ phosphor synthesized via a citrate complex route assisted by microwave irradiation, Solid State Commun. 133 (2005) 657–661, https://doi.org/10.1016/j.ssc.2004.12.046.
[29] T. Yanagida, Study of rare-earth-doped scintillators, Opt. Mater. (Amst.) 35 (2013) 1987–1992, https://doi.org/10.1016/j.optmat.2012.11.002.